RSC Advances

ROYAL SOCIETY OF CHEMISTRY

www.rsc.org/advances

Titaniun amino phosphates : Synthesis, characterization, antimicrobial and cytotoxicity studies.

A. Rajini, A. Ajay kumar, S. Chirra, N. Venkatathri*

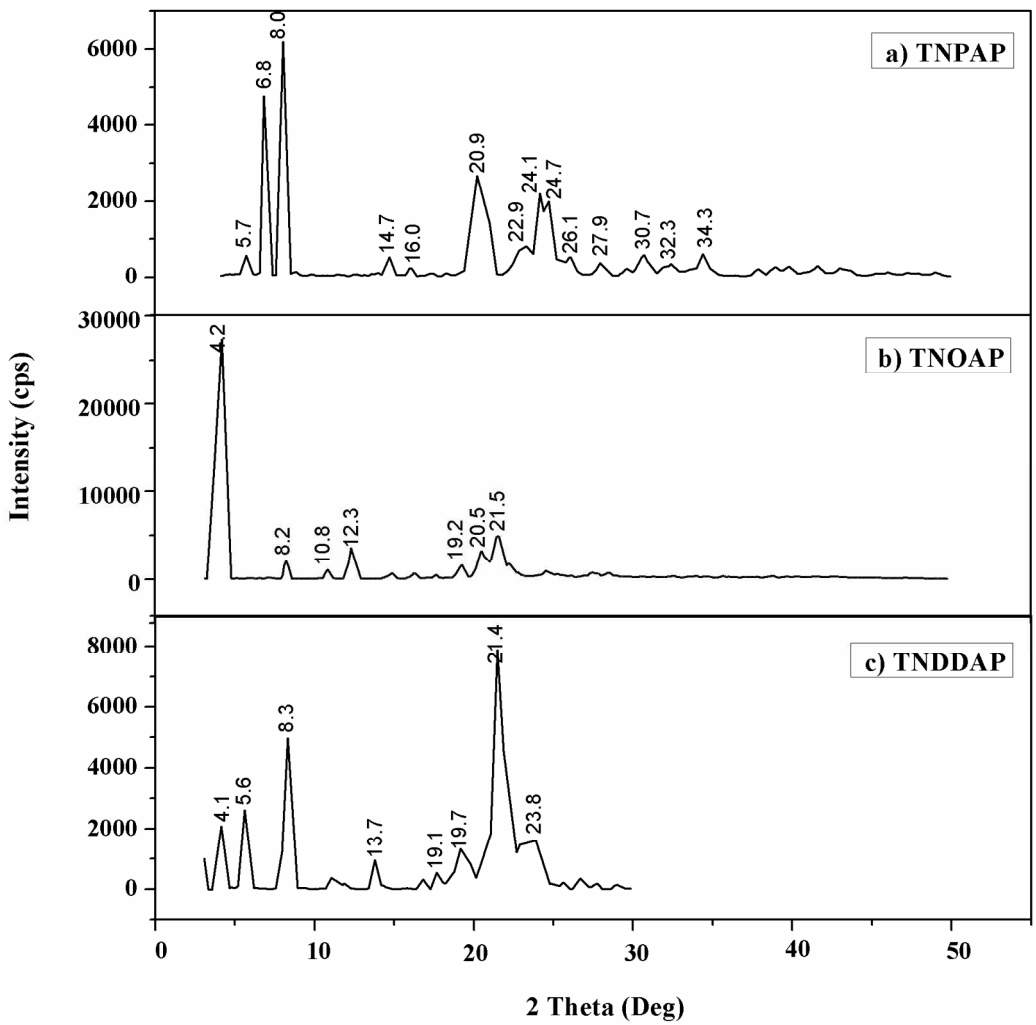

Titaniun amino phosphates were synthesized, characterized in detail and their antimicrobial and cytotoxicity properties were studied.

Titaniun amino phosphates : Synthesis, characterization, antimicrobial and cytotoxicity studies.

A. Rajini, A. Ajay kumar, S. Chirra, N. Venkatathri*

Department of Chemistry, National Institute of Technology, Warangal 506 004, Telangana, India.

(* - corresponding author, E-mail : venkatathrin@yahoo.com and Mobile : +91-94913199

Abstract

Titanium aminophosphates were prepared by using titanium tetraisopropoxide, phosphoric acid and aliphatic amines. The synthesized TNPAP, TNOAP and TNDDAP aminophosphates were characterized by various physicochemical techniques. Powder XRD spectra of titanium aminophosphates suggests the presence of -Ti–O– phase. The % of titanium incorporated into the frameworks of titanium aminophosphates has been confirmed from EDAX analysis. The infrared and Raman spectra infers the presence of peaks due to vibrational bands of Ti–O, P–O, Ti-N, P-N and Ti–O–P, Ti-N-P linkages. The UV–Vis diffuse reflectance spectra reveal the presence of tetrahedral coordination of Ti in the framework. The XPS spectra suggest the presence of –O–Ti–N– or –Ti–N–O– framework in TNPAP. The ^{31}P MASNMR spectra of titanium aminophosphates indicate the presence of environmentally different two tetrahedrally co-ordinated phosphorous atoms in TNPAP framework, other titanium aminophosphates are having unique phosphorous atoms in the framework. The TNPAP, TNOAP and TNDDAP were evaluated for biological applications. TNDDAP only exhibits antimicrobial and nematicidal activity on *M. Incognita* at higher concentrations and incubation time. TNPAP and TNDDAP show λDNA cleavage activity except TNOAP. The *in vitro* anticancer activity has been studied on human cancer cell lines. The TNPAP and TNOAP shows anticancer activity only on HL60

cell line. TNDDAP shows higher anticancer activity against HeLa and MCF7 cell lines and moderately on HL60 cell line.

Keywords : Titanium aminophosphates; synthesis; characterization; antimicrobial; cytotoxicity studies;

Introduction

Titanium is one of the best biomaterials known today [1]. It is one of the early transition metal to be investigated for its antitumor properties. Seventy-six percent of all titanium compounds that have been screened for their anticancer activity are derivatives of bis(β-diketonate)titanium (IV) complexes [2]. Bis(β-diketonate) titanium (IV) complexes are analogues of the titanium drug budotitane (cis-dietoxybis(1-phenylbutane-1,3-dionato)titanium(IV) [3].

Recent advancements in titanium antitumor research open multiple directions to yield more specific, stable to hydrolysis and improved anti-proliferative profile. Ti (IV) can bind to either negatively charged phosphate on the backbone of DNA or to the base nitrogen donors [4].

Phosphate based materials are important in several industrial acid catalysed reactions [5]. In recent years inorganic phosphorous containing materials have received much attention on account of their ability to selectively uptake specific ions, resistance to oxidation, high thermal and chemical stability. In addition, the presence of phosphate in materials seems to enhance catalytic properties, stabilize surface area, crystal phase, improve surface acidity and make the material porous [6].

Research on phosphate based materials with open frameworks is currently in progress due to their applications in catalysis and gas separation [7]. Study of phosphates of transition metals has received great attention in recent years. Phosphate frameworks stabilize reduced

oxidation states, due to its high charge (PO_4^{3-}) and hence favour the formation of anionic frameworks with a high degree of chemical, mechanical and thermal stability.

Aminophosphates are amine and phosphorous based materials. The organic functionality in aminophosphate framework enhances hydrophobicity and shows high activity in base catalyzed reactions [8]. Incorporation of transition metals such as titanium or palladium or vanadium in aminophosphates leads to novel materials with redox properties. In particular, titanium cation Ti^{4+} in framework positions is found to exhibit good activity in shape selective redox reactions. The materials were also evaluated for biological applications such as antimicrobial, nematicidal, DNA cleavage and anticancer activities. Titanium compounds are known for their antimicrobial and cytotoxicity properties. From our earlier report, we came to know that palladium aminophophates are also having the same property due to the modfied electronic environment around palladium [9]. This tend us to extend these studies for titanium aminophosphates. We have observed a better results over these compounds. These compounds are also economic, non-toxic and easy to synthesis compare to the previous one. Further the characterization results shows the morphology, porosity, co-ordination, oxidation state, insertion of titanium over the aminophosphate framework and basic structure of all the synthesized compounds in the present study.

Experimental

Synthesis of titanium aminophosphates was carried out at room temperature. In typical synthesis n-propyl amine (10.9 mL) or n-octyl amine (22.0 mL) or n-dodecyl amine (30.6 mL) was added to 0.05 mL of titanium tetraisopropoxide and was stirred. To this mixture, 1.87 mL of orthophosphoric acid was added and stirred vigorously to yield solid products (0.02 TiO_2: P_2O_5:

8 RNH_2). The products thus obtained were thoroughly washed with ether, dried at 40 °C for about 30 min and ground to fine powder to obtain respective titanium aminophosphates.

Qualitative phase analysis of titanium aminophosphate has been studied using a Bruker AXS D8 Advance diffractometer at room temperature with Cu-Kα X-ray source of wavelength 1.5406 A^o using Si (Li) PSD detector. The morphology and surface elemental composition of the material was investigated using scanning electron microscopy (SEM-EDAX) on a JEOL Model JSM-6390LV. Fourier transform infrared spectroscopy (FT-IR) was recorded on Thermo Nicolet, Avatar 370 spectrophotometer equipped with a pyroelectric detector (DTGS type); a resolution of 4 cm^{-1} was adopted and provided with KBr beam splitter. Dispersive Raman spectroscopy was performed on Bruker senterra at a wavelength of 532 nm using laser radiation as source. The coordination and oxidation state of titanium in titanium aminophosphates were examined by diffuse reflectance UV-Visible spectrophotometer (UV-Vis DRS) on Varian, Cary 5000 in the wavelength range of 175 – 800 nm. . X-ray Photoelectron spectroscopic analysis carried out using ESCA-3000 (VG Scientific, UK) instrument. The ^{31}P magic-angle spinning (MAS) nuclear magnetic resonance (NMR) spectroscopy was performed at room temperature on a Bruker DRX-500 AV-III 500(S) spectrometer, with a spinning rate of 10-12 KHz operating at 121.49 MHz using a 5 mm dual probe. The ^{13}C cross polarization magic-angle spinning (CP-MAS) nuclear magnetic resonance (NMR) spectroscopy was performed at room temperature on a DSX-300 Avance-III 400(L) NMR spectrometer with a spinning rate of 10-12 KHz operating at 75.47 MHz using a 5 mm dual probe.

Results and Discussion

Powder X-ray diffraction patterns of titanium n-propylamino phosphate (TNPAP), titanium n-octylaminophosphate (TNOAP) and titanium n-dodecylaminophosphate (TNDDAP)

are shown in Fig. 1. TNPAP exhibits peaks at 2θ degrees of 22.9°, 24.1°, 26.1°, 27.9° and 30.7° indicates the presence of −Ti−O− linkage [20]. Similarly X-ray diffraction pattern of TNOAP and TNDDAP shows peaks at 2θ degrees of 5.6°, 8.2°, 8.3°, 13.7° and 18.7° corresponding to presence of –Ti–O– with a mesoporous structure [10-12]. TNOAP, TNDDAP exhibits low angle diffraction peaks at 4.1° and 4.2° characteristic of mesoporous structure.

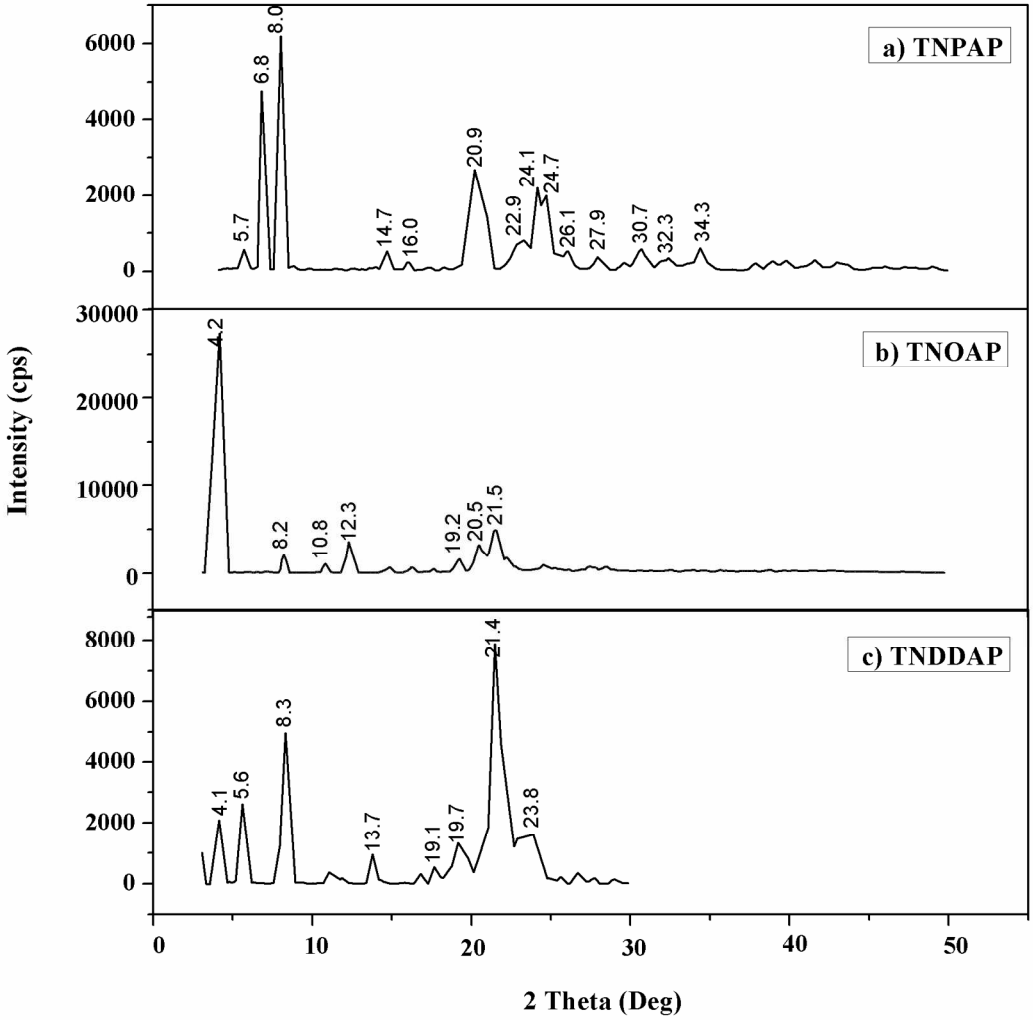

Fig. 1: Low and wide angle powder X-ray diffraction patterns of a) TNPAP, b) TNOAP and c) TNDDAP.

The SEM-EDAX images of TNPAP, TNOAP and TNDDAP are shown in Fig. 2. The SEM images of TNPAP and TNOAP reveal that the materials possess micron sized irregular flakes throughout the surface of the materials. The SEM image of TNDDAP show the material has tubular like morphology. The EDAX analysis of TNPAP, TNOAP and TNDDAP shows the distribution of the constituent elements O, P, N and Ti.

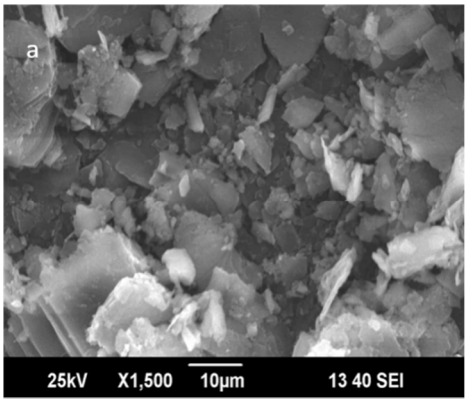

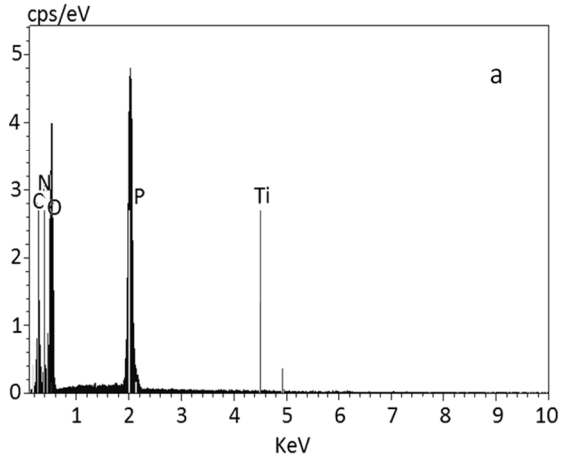

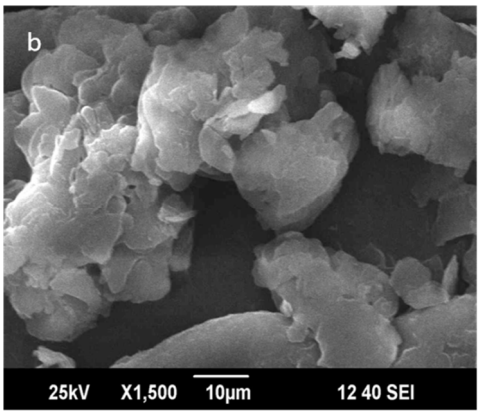

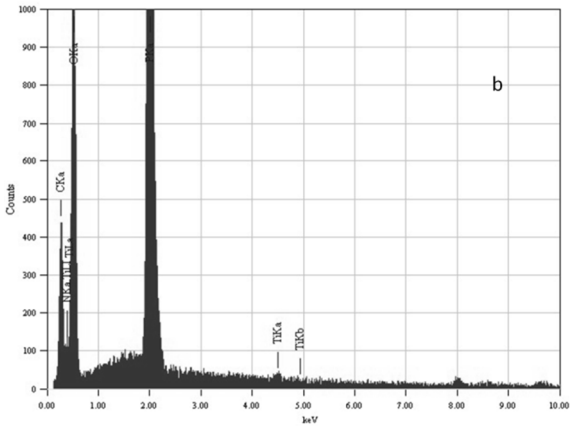

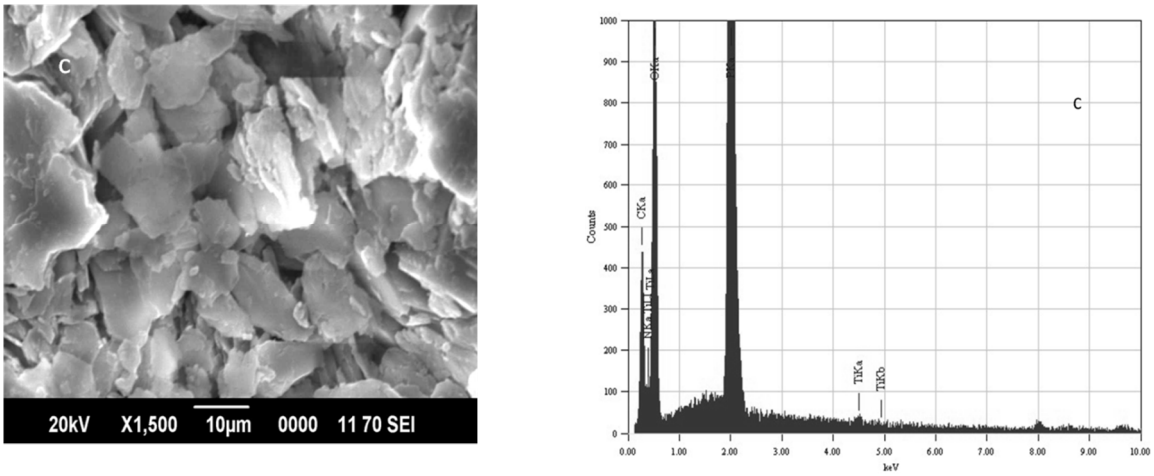

Fig. 2: Scanning electron micrograph – Energy dispersive X-ray analysis of a) TNPAP, b) TNOAP and c) TNDDAP.

The Thermogravimetry / Differential thermal analysis of TNPAP, TNOAP and TNDDAP exhibits continuous weight loss up to 400 °C. This may be due to removal of polymerized molecules. Thereafter, the weight remains constant which indicates the decomposition, combustion and crystallization of organic material present in these materials. DTA shows exothermic peaks for oxidative decomposition of organics and endothermic peaks due to dehydration and evaporation of organic components.

The BET surface area analysis of titanium aminophosphates showed 60, 80 and 100 m^2/g of surface area for TNPAP, TNOAP and TNDDAP respectively. The lesser surface area compared to that reported for zeolites is due to the blockage of pores by alkyl groups present in amines.

The FT-IR spectra of TNPAP, TNOAP and TNDDAP are shown in Fig. 3. TNPAP shows a broad absorption band at 3420 cm^{-1}, which corresponds to O–H or N–H stretching vibrations. The peaks in the range of 3020 - 2850 cm^{-1} corresponds to the alkyl symmetrical and asymmetrical stretching vibrations of amine groups in titanium aminophosphates [13]. Peaks in

the range of 1640 - 1630 cm^{-1} are attributed to O–H bending vibrations of adsorbed water in titanium aminophosphates. Peaks observed at 1469, 1467 cm^{-1} is due to asymmetric deformation vibrations of alkyl group in TNOAP and TNDDAP [14]. The bands at 1079, 1085 cm^{-1} in TNOAP and TNDDAP are attributed to P–O stretching vibrations [15, 16]. The bands at 1038 and 1034 cm^{-1} in TNPAP and TNOAP are due to Ti–O–P stretching vibrations. The bands around 980 cm^{-1} are attributed to vibrational frequencies of P–O group in titanium containing aminophosphates [16]. Peaks at 1240 and 1222 cm^{-1} in TNOAP and TNDDAP correspond to the characteristic absorbance of C–N bonds [17]. The peaks at 887 and 892 cm^{-1} in TNOAP and TNDDAP are due to asymmetric stretching vibrations of P–O–P groups. The peaks at 759, 758 cm^{-1} in TNPAP and TNOAP are attributed to non-bridging Ti–O bond vibrations [18, 19]. The peaks at about 725 and 723 cm^{-1} in TNOAP and TNDDAP are assigned to symmetric stretching vibrations of P–O–P groups. The peaks in the range of 700 - 400 cm^{-1} are attributed Ti–O and Ti–O–Ti vibrations in titanium aminophosphates. The peaks at 538, 492, 530 and 540 cm^{-1} in titanium aminophosphates are attributed to P–O bending vibrations [20, 21].

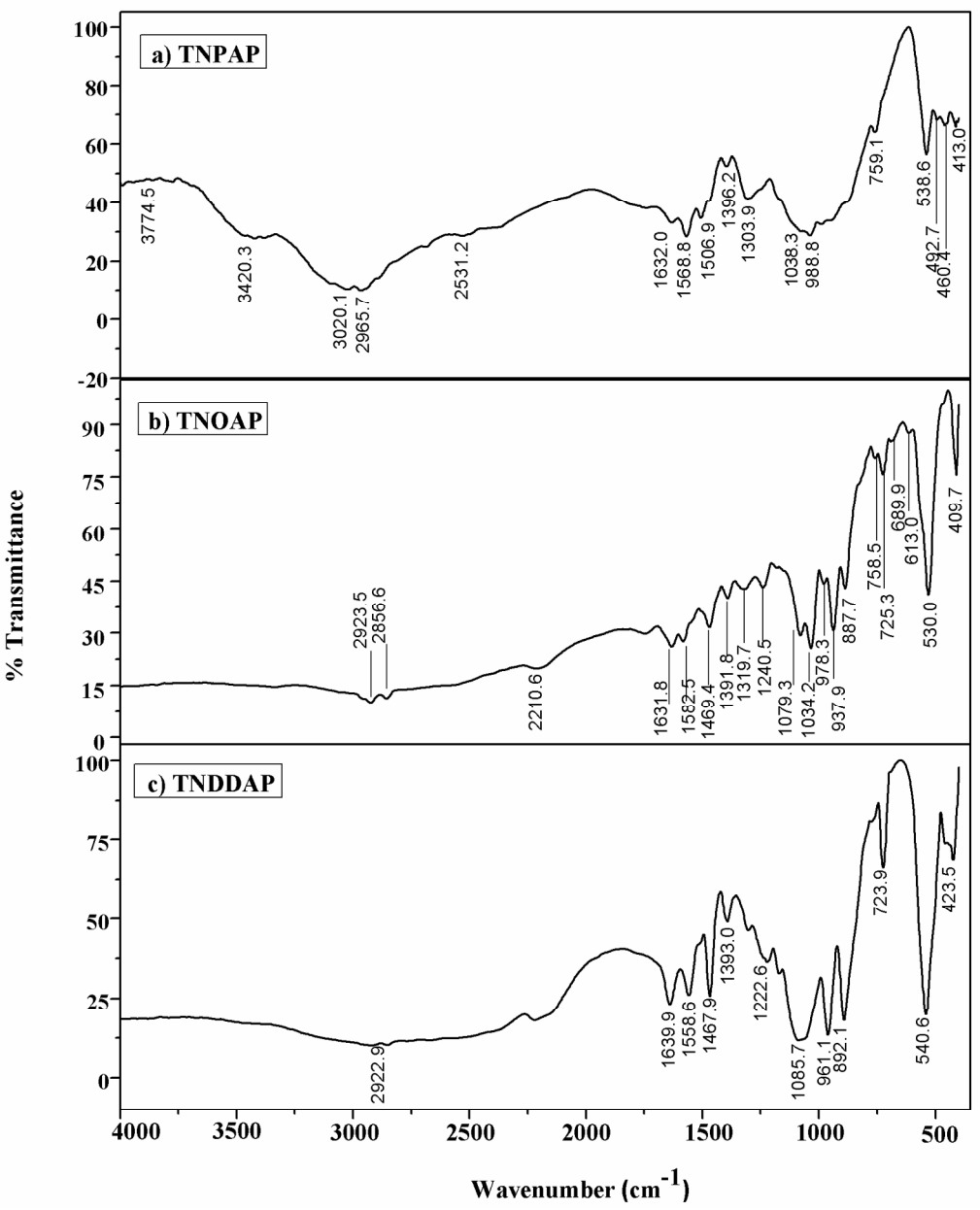

Fig. 3: Fourier transform Infrared spectra of a) TNPAP, b) TNOAP and c) TNDDAP.

The Raman spectra of TNPAP and TNOAP are shown in Fig. 5. Small peaks at 568 cm^{-1} and 939 cm^{-1} in TNPAP corresponds to stretching vibration of Ti−O bond [22.23]. The band

at 1200 cm^{-1} in TNPAP is associated with asymmetric stretching vibration of P−O bond of phosphate group [24].

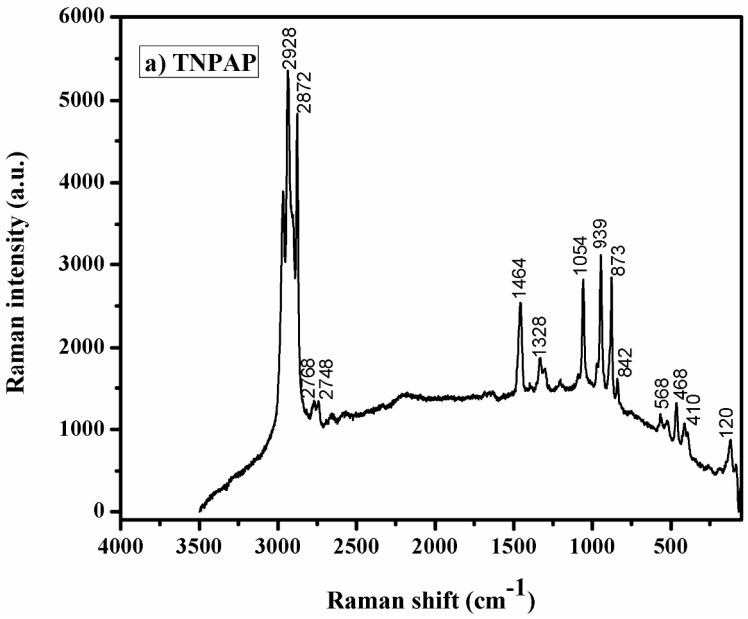

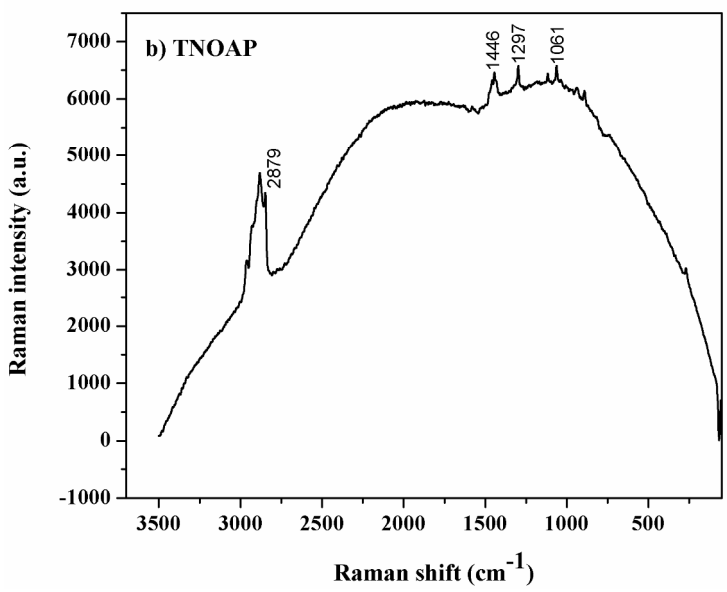

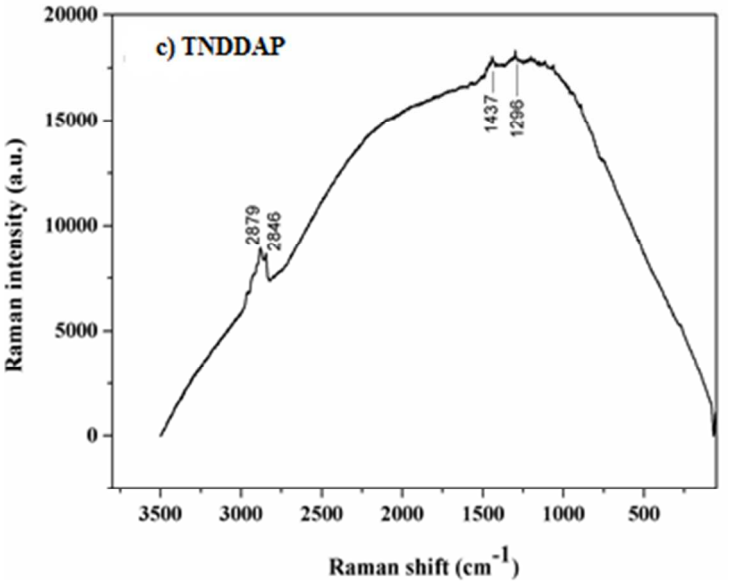

Fig. 4: Dispersive Raman spectra of a) TNPAP, b) TNOAP and c) TNDDAP.

The UV-Visible diffuse reflectance spectra of TNPAP, TNOAP and TNDDAP are shown in Fig. 5. TNPAP and TNDDAP show peaks around 215 nm due to charge transfer transitions between empty 3d-orbital's of Ti (IV) cations and 2p-orbitals of oxygen anions (O^{2-}). The charge transfer transition infers the presence of titanium in tetrahedral coordination. TNPAP, TNOAP and TNDDAP show peaks at 343 and 325 nm respectively. These can be attributed to the existence of titanium in tetrahedral coordination [25,26].

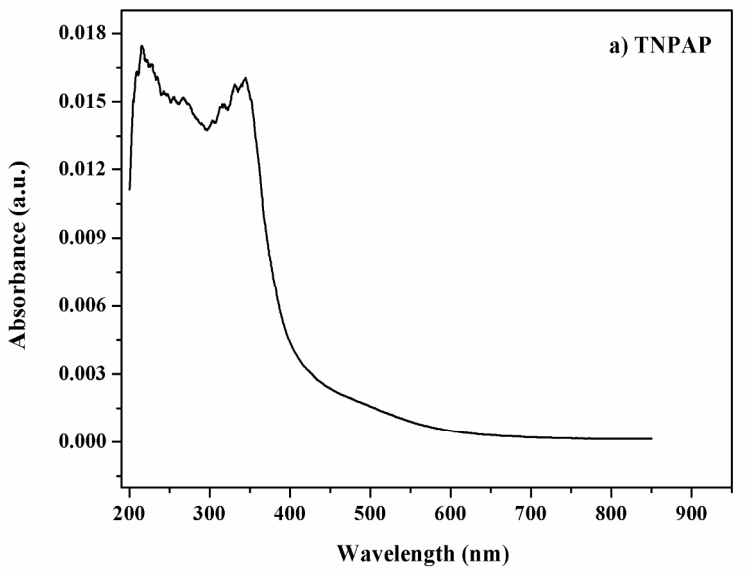

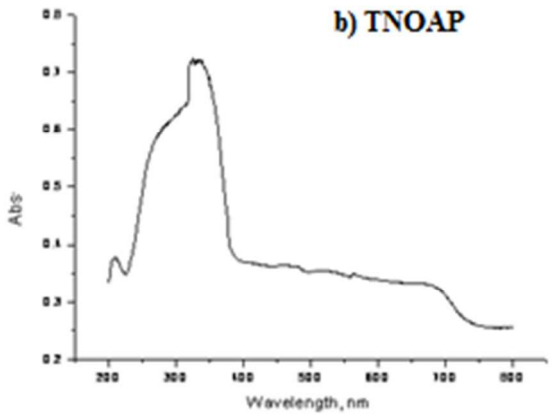

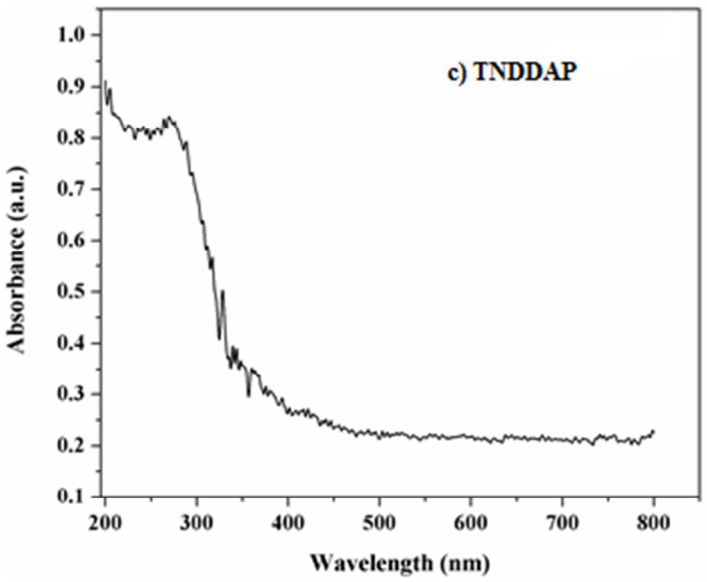

Fig. 5: Ultraviolet - vis DRS spectra of a) TNPAP, b) TNOAP and c) TNDDAP.

The X-ray photo electron (XPS) spectra of carbon, oxygen, nitrogen, phosphorous and titanium ion are shown in Fig. 6. In the XPS spectra of TNPAP, the carbon 1s shows peak at 288.0 eV. This can be attributed to carbon bonded to oxygen, nitrogen and hydrogen respectively [27]. The peak around 534.0 eV corresponds to oxygen 1s binding energy. This is due to chemisorbed water and weakly adsorbed oxygen molecules on the surface. The binding energies of 534.2 eV and 532.4 eV are ascribed to oxygen co-contributed from Ti–O, P–O [28].

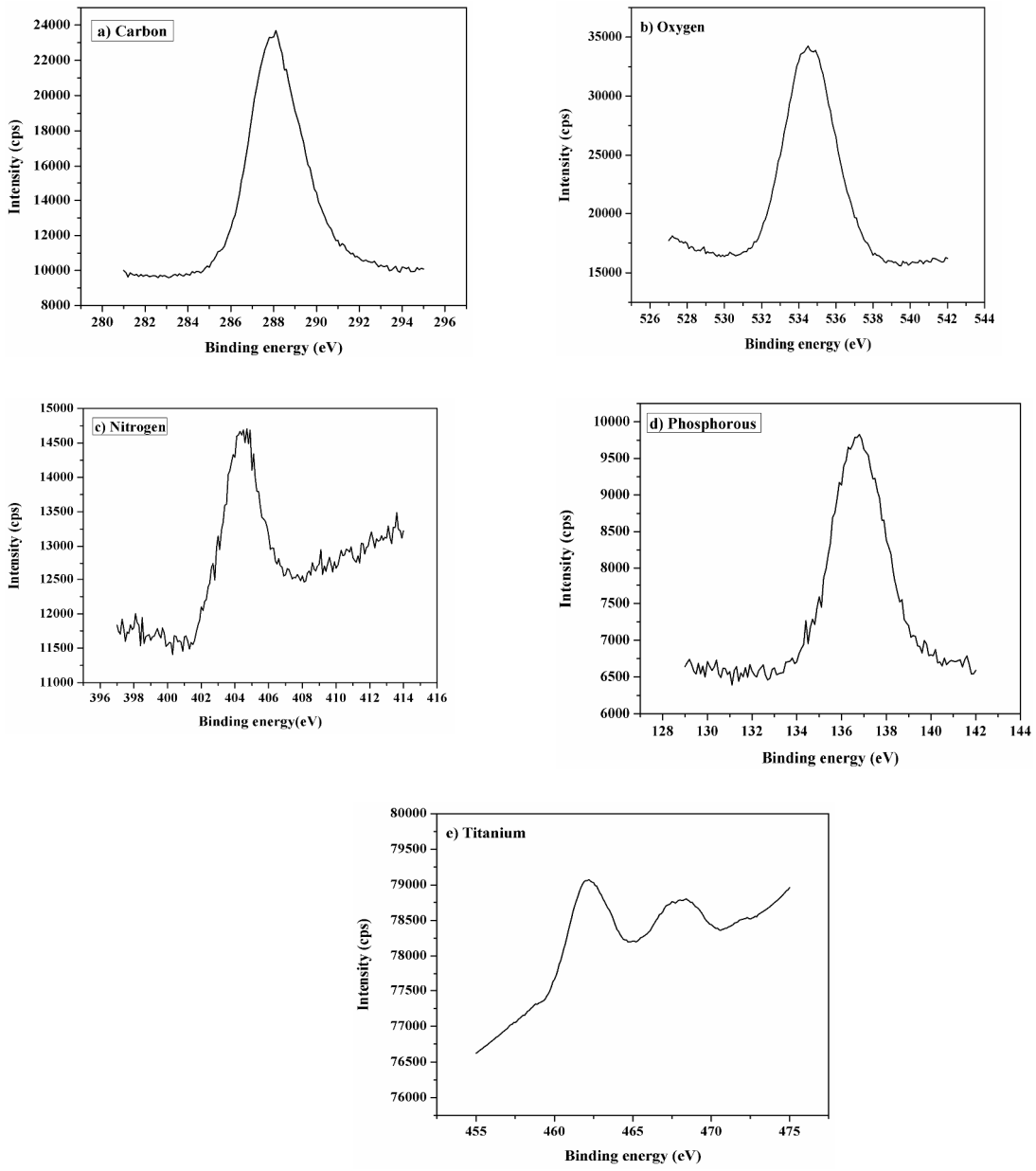

Fig. 6: X-ray photoelectron spectra of a) carbon b) oxygen c) nitrogen d) phosphorous and e) titanium ion in TNPAP.

The peaks at 462 and 468 eV correspond to the binding energies of Ti $2p_{3/2}$ and $2p_{1/2}$ electrons, which is due to nitrogen doped interstitially into the titania matrix [23]. The higher binding energy value of titanium is due to different electronic interaction with nitrogen compared

to oxygen. They suggest considerable modification of the lattice due to N substitution. Titanium binds to nitrogen or oxygen atoms in the lattice to form O–Ti–N or Ti–N–O [28]. The P 2p shows peak at 136.0 eV corresponding to the presence of phosphorous oxide (P_2O_5) in the TNPAP [24].

The ^{31}P MASNMR spectra of TNPAP, TNOAP and TNDDAP are shown in Fig. 7. TNPAP shows peaks at 4.654 ppm and -0.73 ppm with its side bands. The peaks are in 1:3 intensity ratios and suggest the existence of two crystallographically non-equivalent phosphorous atoms. The ^{31}P MASNMR spectra of TNOAP and TNDDAP show peaks at 5.824 and 1.924 ppm. The presence of only one peak in TNOAP and TNDDAP spectra indicates that there is a unique chemical environment of phosphorous atoms. The ^{31}P peaks in the range of -5 to 3 ppm corresponds to the presence of mesoporous crystalline titanium phosphate framework in titanium aminophosphates [30].

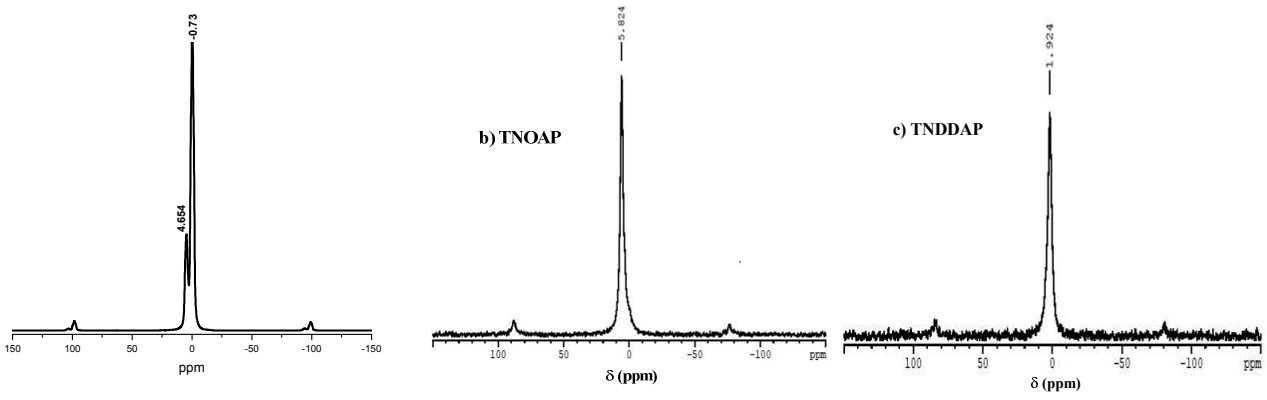

Fig. 7: ^{31}P Magic angle spinning Nuclear magnetic resonance spectra of a) TNPAP, b) TNOAP and c) TNDDAP.

The ^{13}C MASNMR spectra of TNPAP, TNOAP and TNDDAP are shown in Fig. 8. They show peaks at 41.12 and 39.80 ppm, which corresponds to the C_1, carbon bonded to nitrogen atom of amine group. The peaks at 34.46 and 32.12 ppm in TNOAP can be assigned to the C_2 and C_3 carbons linked to C_1 carbon which is directly attached to nitrogen of amine group. The peak at 21.47 ppm in TNPAP can be assigned to the carbon of methylene ($-CH_2-$) group. The peaks at 29.93, 28.37 and 24.49 ppm in TNOAP can be assigned to the carbons of methylene ($-CH_2-$) groups. Peaks at 12.30 and 14.98 ppm in TNPAP and TNOAP can be attributed to the carbon of terminal $-CH_3$ group of amine molecules [14,31].

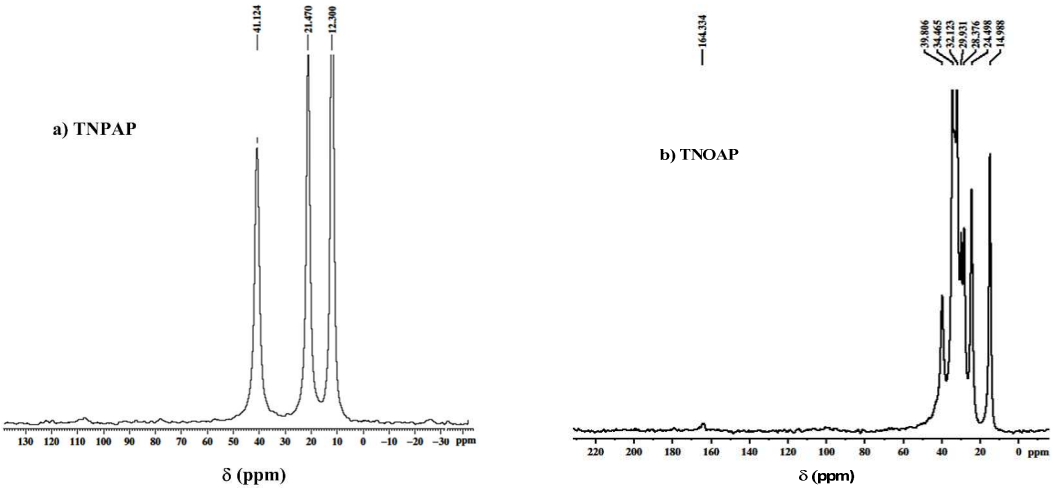

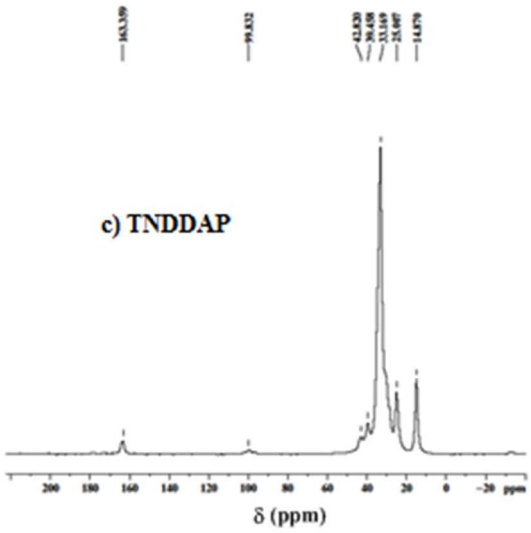

Fig. 8: **^{13}C Magic angle spinning Nuclear magnetic resonance spectra of a) TNPAP, b) TNOAP and c) TNDDAP.**

Based on the above characterization, we have proposed the following plausible mechanism for titanium aminophosphate synthesis and basic structure of the catalysts (Fig. 9). This is a trifunctional catalyst due to the presence of titanium ion (redox), amine (Lewis base) and exchangeable proton (acid) sites. As the reaction is carried out in solvent free condition, there is no residue from the synthesis of catalyst (It means 100% yield). So all the input titanium and amine are present in the basic structure. The presence of solid acid sites are deduced from the proposed structure, which is confirmed by the NaCl ion exchange experiment.

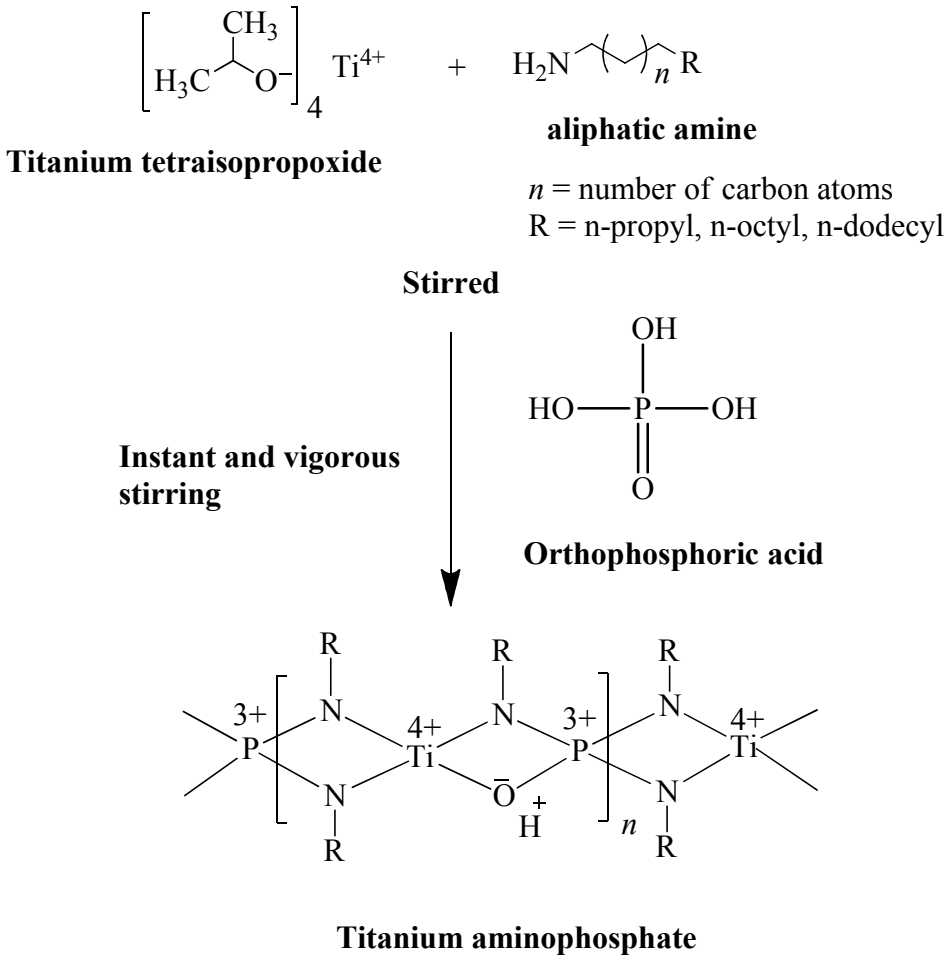

Fig. 9 : Schematic synthesis mechanism and proposed basic structure of titanium aminophosphate.

The titanium containing aminophosphates were evaluated for their *in vitro* antimicrobial activity. The minimum inhibitory concentrations (MIC) of the antimicrobial activity of titanium aminophosphates are presented in Table 1. The results reveal that the TNPAP and TNOAP did not show any antimicrobial activity. The inactivity of TNPAP and TNOAP in antimicrobial activity is due to its low lipophilicity which makes the materials not to penetrate through the lipid membrane. Hence the materials neither block nor inhibit the growth of the microorganism.

TNDDAP exhibits less to moderate activity against all the microbial strains tested when compared with the standard antibiotics ampicillin and clotrimazole.

TNDDAP inhibits the growth of bacteria and the MIC values were found in the range 14 to 26 μg mL^{-1}. The TNDDAP exhibits the maximum anti-bacterial activity against *S. aureus* with MIC value of 14 μg mL^{-1} and moderate against *P. fluorescens* with MIC value of 26 μg mL^{-1}. The MIC value against *E. coli* was found to be 18 μg mL^{-1}. The anti-fungal activity of TNDDAP against *C. albicans* shows a MIC value of 16 μg mL^{-1}.

The variation in length of the alkyl chain of amine is thought to influence the extent of antimicrobial activity [32]. It is also reported in the literature that the antimicrobial activity depends on the properties of amine side chains [33]. The longer alkyl chain amine in TNDDAP shows higher antimicrobial activity than shorter chains in TNPAP and TNOAP.

The electron releasing groups of dodecylamine in TNDDAP reduces the polarity by partial sharing of its charge with the positive charge of the titanium ion [34,35]. Further, it increases the electron delocalization and stabilizes the whole framework and enhances the lipophilicity. The enhanced lipophilicity favours the materials to penetrate into lipid membranes of the bacterial cell more efficiently [36,37].

Further, the activity of TNDDAP can also be explained on the basis of overtones concept and chelation theory [38,39]. According to overtones concept of cell permeability, the lipid membrane that surrounds the cell, favors the passage of only lipid soluble materials. Liposolubility is an important factor which controls the antimicrobial activity. The activity is due to the lipophilic nature of the material arising from chelation [40].

Table 1: Minimum inhibitory concentration values (µg mL^{-1}) of antimicrobial activity of titanium containing aminophosphates

Compound	*B. subtilis*	*S. aureus*	*P. vulgaris*	*P. fluorescens*	*E. coli*	*C. albicans*
TNPAP	-	-	-	-	-	-
TNOAP	-	-	-	-	-	-
TNDDAP	16	14	22	26	18	16
Ampicillin	14	12	16	16	16	-
Clotrimazole	-	-	-	-	-	10

The nematicidal activity of titanium containing aminophosphates was evaluated against *Meloidogyne incognita* with different concentrations after 24 and 48 h of incubation time and the results are presented in Table 2.

Table 2: Nematicidal activity (% mortality) observed against different concentrations of titanium containing aminophosphates on *Meloidogyne incognita*. Effect of incubation time on % mortality

Compound	24 h			48 h		
	Concentration (µg mL^{-1})					
	250	150	50	250	150	50
TNPAP	-	-	-	-	-	-
TNOAP	-	-	-	-	-	-
TNDDAP	44	32	18	78	63	40

The results reveal that, TNPAP and TNOAP did not show any activity. TNDDAP exhibits 78% mortality in 250 μg mL^{-1} concentration after 48 h exposure indicating the good activity. Aliphatic amines having the carbon chain length of 9 to 35 are found to be highly lethal to nematodes and parasites [41]. However, the activity of TNDDAP depends on concentration and time. *i.e.,* the activity was higher at high concentrations and was found to increase with incubation time. The percentage mortality in the presence of TNDDAP was increased from 18 to 78% with increase in concentration from 50 to 250 μg mL^{-1} and incubation time from 24 to 48 h.

The DNA cleavage activity of titanium containing aminophosphates was investigated using agarose gel electrophoresis on λDNA. The gel electrophoresis image of titanium aminophosphates is shown in Fig. 10. Control DNA (In Fig. Lane C) does not show any cleavage of DNA in its lane. $FeSO_4$ (In Fig. Lane +ve) was used as standard, complete disappearance of bands was observed in its lane, indicating the DNA cleavage. The lanes TNPAP and TNDDAP clearly show the complete disappearance of control bands. Lane TNOAP does not show any DNA cleavage. It indicates that the titanium aminophosphates exhibit significant DNA cleavage without using any external reagents like H_2O_2. The DNA cleavage activity of titanium aminophosphates may be due to electrostatic interactions of titanium with the base pairs of λDNA molecule.

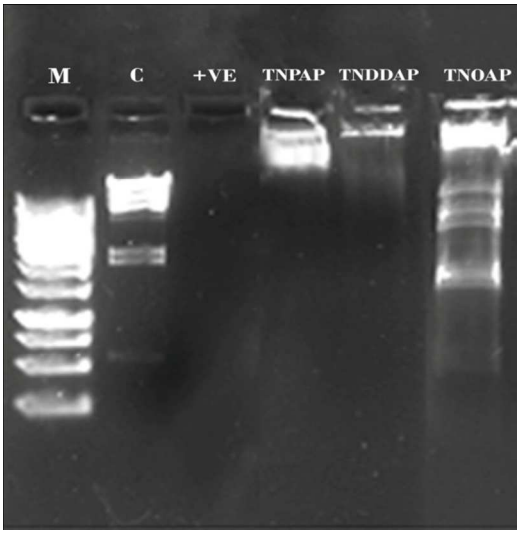

Fig. 11: **Gel electrophoresis image of titanium containing aminophosphates: DNA cleavage activity of titanium containing aminophosphates against λDNA:** Lane M. DNA + marker, lane C. DNA alone, lane +ve. DNA + $FeSO_4$, lane TNPAP. DNA + TNPAP, lane TNDDAP. DNA + TNDDAP, lane TNOAP. DNA + TNOAP.

Synthesized titanium aminophosphates TNPAP, TNOAP and TNDDAP were evaluated for *in vitro* anticancer activity against human cancer cell lines such as MCF7, HeLa and HL60 by sulforhodamine B assay. The growth inhibition of 50% (GI50) values of TNPAP, TNOAP, TNDDAP and standard drug doxorubicin obtained against selected cancer cell lines are shown in Table 3.

Table 3: Anticancer activity of titanium containing aminophosphates on human HeLa, MCF7 and HL60 cancer cell lines using sulforhodamine B assay

Cell lines	GI50		GI50		GI50	
	TNPAP	**Doxorubicin**	**TNOAP**	**Doxorubicin**	**TNDDAP**	**Doxorubicin**
HeLa	>80	<10	>80	<10	10.6	<10

MCF7	>80	<10	>80	<10	13.2	<10
HL60	12.7	<10	48.3	<10	39.8	<10

Note: GI50 (μ Molar) = growth inhibition of 50% (GI50) drug concentration resulting in a 50% reduction in the net protein increase, doxorubicin = positive control compound, HeLa = cervix, MCF7 = breast and HL60 = leukemia cancer cell lines.

Estimation based on GI50 values shows that all the titanium containing aminophosphates exhibit anticancer activity. TNPAP and TNOAP exhibit activity exclusively on HL60 cell line with GI50 values of 12.7 and 48.3 μg mL^{-1}. All the three materials have no effect on the viability of HeLa and MCF7 cell lines. The low anticancer activity of TNPAP and TNOAP is due to its low solubility or they are not taken up by the cell lines [42]. Among the three compounds tested, TNDDAP exhibits higher anticancer activity on HeLa (Fig. 3.18a) and MCF7 (Fig. 3.18b) cell lines with GI50 values of 10.6 and 13.2 μg mL^{-1} and moderate activity on HL60 cell line (Fig. 3.18c) with a GI50 value of 39.8 μg mL^{-1}.

The anticancer activity of the titanium aminophosphates depends on lipophilicity and membrane permeability because they have to cross the hydrophobic cell membrane to exhibit their activity. Previous studies on pharmacokinetics revealed that lipophilicity of the compounds increases as carbon chain length increases. Increased lipophilicity leads to better permeability through cell membrane and results in increased potency [43,44]. The TNDDAP with 12 carbon alkyl chain is having higher lipophilicity passes rapidly through permeable membrane compared to 3 and 8 carbon atoms which contains TNPAP and TNOAP. Consequently TNDDAP exhibits highest anticancer activity. These results clearly indicate that the length of alkyl chain in the amine plays an important role in determining the anticancer activity of titanium containing

aminophosphates. It was observed that the length of the alkylchain coordinated to the titanium is a significant factor which influencing the toxicity of the compounds.

The activity of titanium containing aminophosphates in anticancer activity can be understood due to following reasons. The high oxidation state of Ti(IV) in titanium aminophosphates may prevent oxidation in the body. The open framework, and neutral charge on the titanium aminophosphates allows the passive diffusion of titanium ions into cancer cells. Presence of amino groups in titanium containing aminophosphates also influences the anticancer activity. Results indicate that the compounds should possess at least one N–H bond linkage in order to exhibit anticancer activity.

Amino groups in titanium aminophosphates may increase the electron density on Ti (IV) centre, stabilize it and enhance its interaction with the Lewis base sites of DNA [86]. Previous studies on anticancer reported that titanium ions may intercalate with the DNA base pairs and allow the titanium–DNA interactions. This results in passive diffusion of titanium ions into the cancer cells and show anticancer activity [45]. These studies indicate that the titanium aminophosphates bind strongly to the phosphate groups of nucleotides and lead to anticancer activity [46]. This may be due to higher efficiency of bonding of titanium to phosphorous.

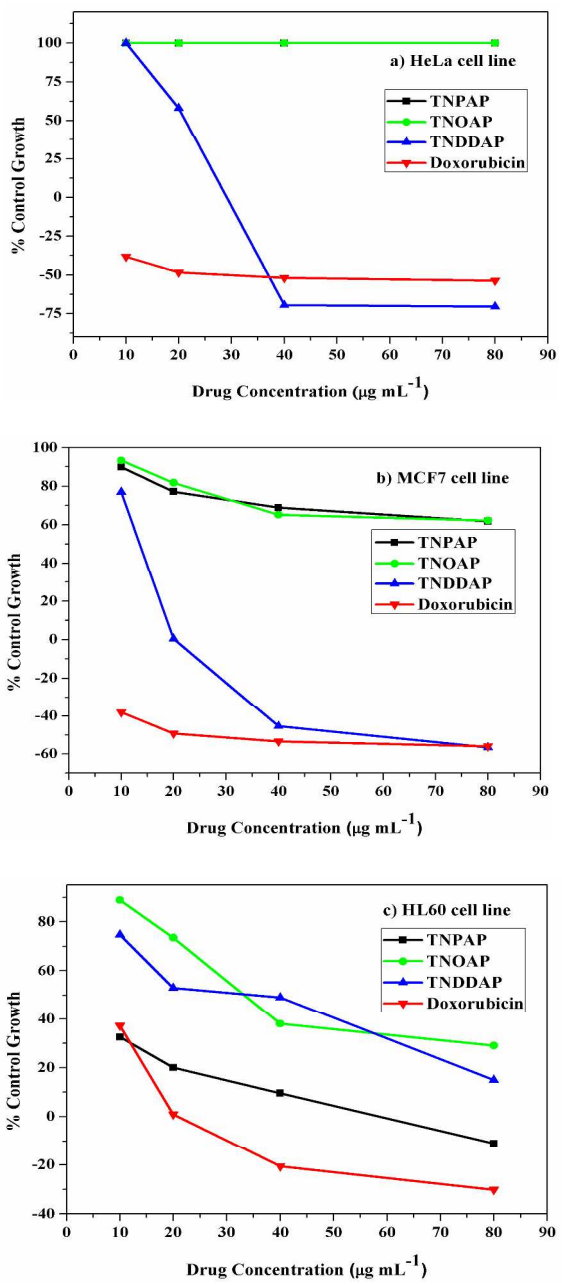

Fig. 11 : Anticancer activity of titanium containing aminophosphates on human cancer cell lines a) HeLa, b) MCF7 and c) HL60 using sulforhodamine B assay.

Conclusions

Titanium aminophosphates were prepared by employing titanium tetraisopropoxide, phosphoric acid and aliphatic amines. The synthesized TNPAP, TNOAP and TNDDAP aminophosphates were characterized by various physicochemical techniques. Powder XRD spectra of titanium aminophosphates suggests the presence of -Ti–O– phase. The % of titanium incorporated into the frameworks of titanium aminophosphates has been confirmed from EDAX analysis. The infrared and Raman spectra infers the presence of peaks due to vibrational bands of Ti–O, P–O and Ti–O–P linkages. The UV–Vis diffuse reflectance spectra reveal the presence of tetrahedral coordination of Ti in the framework. The XPS spectra suggest the presence of –O–Ti–N– or –Ti–N–O– framework in TNPAP. The ^{31}P MASNMR spectra of titanium aminophosphates indicate the presence of crystalline titanium phosphate framework. The TNPAP, TNOAP and TNDDAP were evaluated for biological applications. TNDDAP only exhibits antimicrobial and nematicidal activity on *M. Incognita* at higher concentrations and incubation time. TNPAP and TNDDAP show λDNA cleavage activity except TNOAP. The *in vitro* anticancer activity has been studied on human cancer cell lines. The TNPAP and TNOAP shows anticancer activity only on HL60 cell line. TNDDAP shows higher anticancer activity against HeLa and MCF7 cell lines and moderately on HL60 cell line.

Acknowledgement

The authors A.R., A.A.K and S.C. thank MHRD, New Delhi for a research fellowship.

3.7: References

[1] S. Rafique, M. Idrees, A. Nasim, H. Akbar, A. Athar, Biotechnol. Mol. Biol. Rev. 5 (2010) 38.

[2] R. Huang, A. Wallqvist, D.G. Covell, Biochem. Pharmacol., 69 (2005) 1009.

[3] B.K. Keppler, C. Friesen, H. Vongerichten, E. Vogel, Met. Complexes Cancer Chemother. (1993) 297.

[4] H.Z. Sun, H.Y. Li, P.J. Sadler, Chem. Rev. 99 (1999) 2817.

[5] S.K. Samantaray, T. Mishra, K.M. Parida, J. Mol. Catal. A: Chem. 156 (2000) 267.

[6] S.K. Samantaray, K.M. Parida, J. Mol. Catal. A: Chem. 176 (2001) 151.

[7] A.K. Cheetham, G. Ferey, T. Loiseau, Angew. Chem. Int. Ed. Engl. 38 (1999) 3268.

[8] C. Berlini, M. Guidotti, G. Moretti, R. Psaro, N. Ravasio, Catal. Today 60 (2000) 219.

[9] A. Rajini, A. Ajay kumar, S. Chirra, N. Venkatathri, RSC Advances, 5 (2015) 66956

[10] K. Khosravi, M.E. Hoque, B. Dimock, H. Hintelmann, C.D. Metcalfe, Anal.

Chim. Acta. 713 (2012) 86.

[11] D.M. Antonelli, J.Y. Ying, Angew. Chem. Int. Ed. Engl. 34 (1995) 2014.

[12] A.R. Khataee, M.B. Kasiri, J. Mol. Catal. A: Chem. 328 (2010) 8.

[13] M. Nagao, Y. Suda, Langmuir 5 (1989) 42.

[14] L. Zhang, J. Xu, G. Hou, H. Tang, F. Deng, J. Colloid Interface Sci. 311 (2007) 38.

[15] K.M. Parida, M. Acharya, S.K. Samantaray, T. Mishra, J. Colloid Interface Sci. 217 (1999) 388.

[16] S.F. Lincoln, D.R. Stranks, Aust. J. Chem. 21 (1968) 37.

[17] X.A. Zhao, C.W. Ong, Y.C. Tsang, Y.W. Wong, P.W. Chan, C.L. Choy, Appl. Phys. Lett. 66 (1995) 2652.

[18] S. Sakka, F. Miyaji, K. Fukumi, J. Non-Cryst. Solids 112 (1989) 64.

[19] N.G. Chernorukov, I.A. Korshunov, M.I. Zhuk, Russ. J. Inorg. Chem. 27 (1982) 1728.

[20] A. Nilchi, M.G. Maragheh, A. Khanchi, M.A. Farajzadeh, A.A. Aghaei, J. Radio. Nucl. Chem. 261 (2004) 393.

[21] B.B. Sahu, K. Parida, J. Colloid Interface Sci. 248 (2002) 221.

[22] C. Schmutz, P. Barboux, F. Ribot, F. Taulelle, M. Verdaguer, C. Fernandez-Lorenzo, J. Non-Cryst. Solids, 170 (1994) 250.

[23] X. Gao, I.E. Wachs, Catal. Today 51 (1999) 233.

[24] L.A. Farrow, E.M. Vogel, J. Non-Cryst. Solids 143 (1992) 59.

[25] S. Jhung, Y.S. Uh, H. Chon, Appl. Catal. 62 (1990) 61.

[26] J. Kornatowski, B. Wichterlova, M. Roswadowski, W.H. Baur, Stud. Surf. Sci.

Catal. 84A (1994) 117.

[27] H.-F. Yu, S.-T. Yang, J. Alloys Compd. 492 (2010) 695.

[28] K.M. Parida, N. Sahu, J. Mol. Catal. A: Chem. 287 (2008) 151.

[29] C. Di Valentin, E. Finazzi, G. Pacchioni, A. Selloni, S. Livraghi, M.C. Paganini, E. Giamello, Chem. Phys. 339 (2007) 44.

[30] E. Jaimez, A. Bortun, G.B. Hix, J.R. Garcia, J. Rodrıguez, R.C.T. Slade, J. Chem. Soc., Dalton Trans. (1996) 2285.

[31] A. Hayashi, H. Nakayama, M. Tsuhako, Solid State Sci. 11 (2009) 1007.

[32] A.M. Bonilla, M.F. Garcia, Prog. Polym. Sci. 37 (2012) 281.

[33] B. Keshavan, H. Kempe Gowda, Turk. J. Chem. 26 (2002) 237.

[34] K. Kralova, K. Kissova, O. Svajlenova, J. Vanco, Chem. Pap. 58 (2000) 357.

[35] K. Shanker, R. Rohini, V. Ravinder, P.M. Reddy, Y.P. Ho, Spectrochim. Acta Part A: 73 (2009) 205.

[36] N.M.A. Atabay, B. Dulger, F. Gucin, Eur. J. Med. Chem. 40 (2005) 1096.

[37] B.G. Tweedy, Phytopathology 55 (1964) 910.

[38] M.N. Patel, B.S. Bhatt, P.A. Dosi, Z. Anorg. Allg. Chem. 638 (2012) 152.

[39] S.D.L. Yadav, S. Singh, Ind. J. Chem. B 40 (2001) 440.

[40] M.J. Thompson, Baltimore; J. Feldmesser; W.E. Robbins, U.S. Patent 1977.

[41] J.K. Seydel, K.J. Schaper, in Pharmacokinetics: Theory and Methodology, eds M. Rowland, G. Tucker, Pergamon Press, New York (1986) 311.

[42] Richard B. Silverman, Mark W. Holladay, The Organic Chemistry of Drug Design and Drug Action, Academic Press 3rd Edition (1992) 422.

[43] S. Toon, M. Rowland, J. Pharmacol. Exp. Ther. 225 (1983) 752.

[44] S. Gomez Ruiz, G.N. Kaluderovic, S. Prashar, D. Polo-Ceron, M. Fajardo, Z. Zizak, T.J. Sabo, Z.D. Juranic, J. Inorg. Biochem. 102 (2008) 1558.

[45] C. Pampillon, J. Claffey, K. Strohfeldt, M. Tacke, Eur. J. Med. Chem. 43 (2008) 122.

[46] M.L. Guo, Z.J. Guo, P.J. Sadler, J. Biol. Inorg. Chem. 6 (2001) 698.